THE ASTROPHYSICAL JOURNAL, 468:225–230, 1996 September 1

THE DOUBLE INFRARED SOURCE TOWARD THE SOFT GAMMA-RAY REPEATER SGR 1900+14

F. J. VRBA,[1] C. B. LUGINBUHL,[1] K. C. HURLEY,[2] P. LI,[2] S. R. KULKARNI,[3] M. H. VAN KERKWIJK,[3] D. H. HARTMANN,[4] L. E. CAMPUSANO,[5,6] M. J. GRAHAM,[6,7] R. G. CLOWES,[6,7] C. KOUVELIOTOU,[8] R. PROBST,[9] I. GATLEY,[9] M. MERRILL,[9] R. JOYCE,[9] R. MENDEZ,[10] I. SMITH,[11] AND A. SCHULTZ[12]

Received 1996 February 2; accepted 1996 March 26

ABSTRACT

We report the results of an extensive set of optical and near-infrared photometry and spectroscopy of the double infrared source reported by Hartmann et al. (1995) as a potential counterpart for the Galactic soft gamma-ray repeater SGR 1900+14. These objects are found to be variable but otherwise normal M5 supergiant stars at a distance of ≈12–15 kpc and extinguished by $A_V \approx 19.2$ mag, primarily by the general interstellar medium. We argue that the supergiants are likely gravitationally bound. These stars are positionally coincident with both quiescent X-ray and *IRAS* sources, suggestive of a yet-undetected third component to the system which may be responsible for the SGR.

Subject headings: gamma rays: bursts — gamma rays: observations — supergiants

1. INTRODUCTION

The three known soft gamma-ray repeaters (SGRs) are characterized by short and repetitive outbursts with distinctly soft X- and gamma-ray spectra and thus constitute a unique subclass of high-energy transients, thought to originate from Galactic compact objects (Norris et al. 1991). SGR 0525−66 is the source of the well-known 1979 March 5 event and has a position consistent with the N49 supernova remnant in the Large Magellanic Cloud (Cline et al. 1982). Apart from a soft X-ray source (Rothschild, Kulkarni, & Lingenfelter 1994), this object has no known counterpart (Dickel et al. 1995). SGR 1806−20 is located toward the Galactic center and is the most prolific SGR burster (Kouveliotou et al. 1994). It has been associated with the radio "plerionic" supernova remnant G10.0−0.3 (Kulkarni et al. 1994) and a very luminous blue star (Kulkarni et al. 1995; van Kerkwijk et al. 1995).

The third and least active (Kouveliotou et al. 1993) is SGR 1900+14, which has recently been localized to a region in the Galactic plane near the revised KONUS error box using the network synthesis (NS) method (Hurley et al. 1994). This position is just outside the outer radio contours of the Galactic supernova remnant G42.8+0.6, which previously was suggested to be associated with the SGR (Vasisht et al. 1994). In addition, *ROSAT* All Sky Survey (Vasisht et al. 1994) and *ROSAT* HRI (Hurley et al. 1995) X-ray sources have been noted just outside of the NS localization. We have carried out an optical and near-infrared search of the NS region for a counterpart to SGR 1900+14 which led to the discovery of a double infrared source (Hartmann et al. 1995). The infrared source is spatially coincident with an X-ray source; *ROSAT* HRI, *EUVE*, and VLA observations of which are presented in Hurley et al. (1996). We report here the optical and near-infrared photometric and spectroscopic properties of the double infrared source.

2. OBSERVATIONS

During 1994 June–July *UBVI* CCD imaging was obtained at the USNO 1.0 and 1.55 m telescopes of a region centered upon and covering many times the area of the NS localization of SGR 1900+14 (Hurley et al. 1994). These frames revealed two very red sources (denoted "A" and "B" in the main panel of Fig. 1), separated by 3″.373 ± 0″.001, with $I \approx 18$, but undetected in the *V*, *B*, or *U* to limiting magnitudes of ≈24.5, 24.0, and 23.0, respectively. At 2″.438 ± 0″.002 from object B lies a fainter object which we denote as "C." During the same period, near-IR array observations in the *J*, *H*, and *K* bands using the SQIID IR camera at the KPNO 1.3 m telescope and IRCAM at the USNO 1.55 m telescope revealed A and B to have steeply rising energy distributions toward longer wavelengths (Hartmann et al. 1995). The positions of the objects (Table 1) are coincident with an *IRAS* source (van Paradijs et al. 1996), which also has a steeply rising energy spectrum, and probably with the peak emission of the *ROSAT* HRI images (Hurley et al. 1995, 1996). These circumstances prompted us to carry out an extensive set of optical, near-IR, and spectroscopic observations to understand the nature of objects A, B, and C.

Between 1994 July and 1995 October I_{KC} band CCD photometry was carried out at the USNO 1.55 m telescope

[1] US Naval Observatory, Flagstaff Station, P.O. Box 1149, Flagstaff, AZ 86002-1149.
[2] Space Sciences Laboratory, University of California, Berkeley, CA 94720-7450.
[3] California Institute of Technology, Department of Astronomy, 105-24, Pasadena, CA 91125.
[4] Clemson University, Department of Physics and Astronomy, Clemson, SC 29634-1911.
[5] Observatorio Astronómico Cerro Calán, Departamento de Astronómia, Universidad de Chile, Casilla 36-D, Santiago, Chile.
[6] Visiting Astronomer, Cerro Tololo Inter-American Observatory. CTIO is operated by AURA, Inc. under cooperative agreement with the National Science Foundation.
[7] Centre for Astrophysics, University of Central Lancashire, Preston, PR1 2HE, England, UK.
[8] NASA Marshall Space Flight Center, ES-62, Huntsville, AL 35812.
[9] Kitt Peak National Observatory, P.O. Box 26732, Tucson, AZ 85726-6732.
[10] European Southern Observatory, Karl-Schwarzschild-Strasse 2, 85748 Garching bei München, Germany.
[11] Rice University, Space Physics and Astronomy, P.O. Box 1892, Houston, TX 77251-1892.
[12] NASA-Ames Research Center, MS 245-6, Moffett Field, CA 94035-1000.

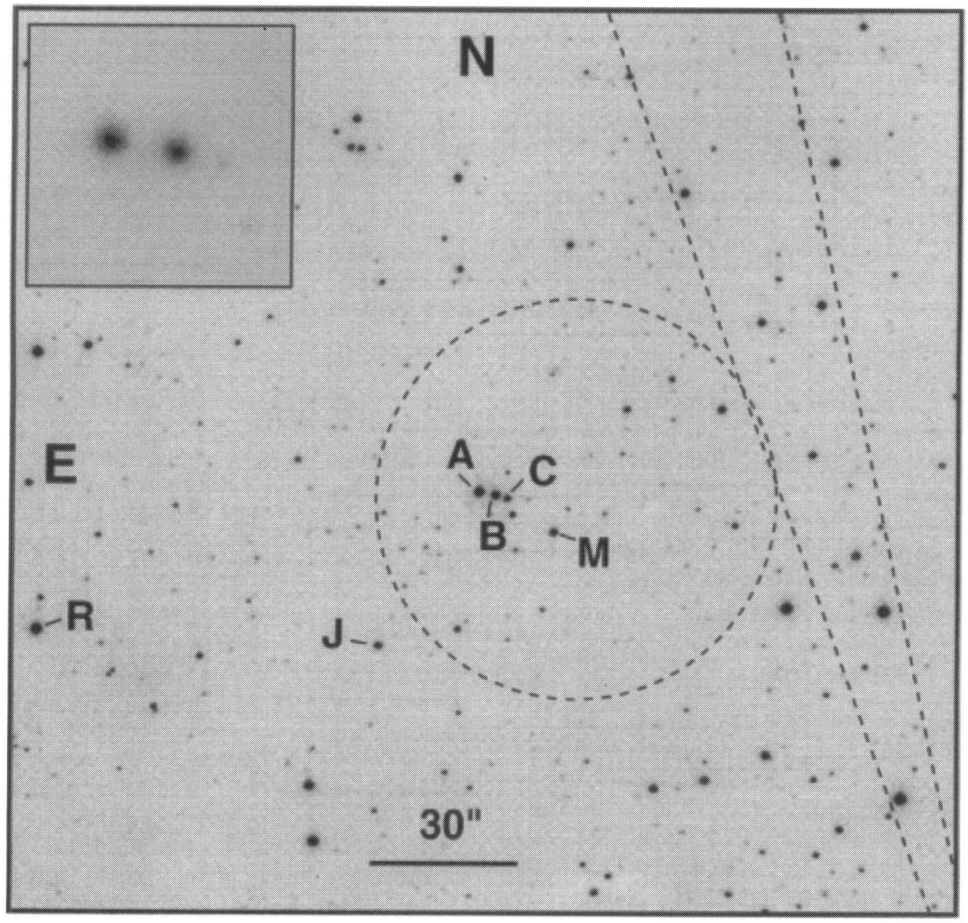

FIG. 1.—A portion of an *I*-band 300 s exposure taken with a Tek 2k CCD at the USNO 1.55 m telescope on UT 1995 May 4 is shown. This frame shows the spatial relationship between stars A, B, and C and stars J, M, and R used for an astrometric reference frame in this paper. The circle shows the approximate boundary of the *ROSAT* HRI X-ray source image described by Hurley et al. (1996). The lines show a portion of the NS localization of SGR 1900+14 (Hurley et al. 1994). The orientation and scale of the CCD frame are indicated on the figure. An example KPNO 4 m telescope COB *K*-band image, as explained in the text, is shown in the insert.

on 12 nights with as many as eight frames covering several hours during each night. The nightly means of the *I*-band observations along with the A and B magnitude differences are listed in Table 2 and plotted in Figure 2. The observations show that both A and B were variable, with amplitudes of 0.18 and 0.35 mag, respectively, while C was constant to within 0.02 mag. During each night, we found no variability greater than 0.02 mag for any of these objects. Since C is fainter than either A or B, and B is closer to C than A, the constancy of C demonstrates the reliability of the photometry for all of these narrowly separated objects.

Due to the extremely red nature of objects A and B, the KPNO SQIID camera IR measurements were so saturated as to be useless for photometry. While USNO IRCAM *JHK* observations taken at the maximum frame rate (0.62 s) on two different nights were marginally saturated for the central few pixels of the A and B images, photometry could be accomplished by fitting to the point spread function (PSF) wings, although with less accuracy than otherwise expected for such bright objects (see Table 3). The resultant *J*-band A and B photometry is also plotted onto the *I*-band A and B photometry in Figure 2 and shows, despite the comparison of different bandpasses, that the variation of the sources in the near-IR is consistent with that in the *I*-band. As a further check, *K*-band observations using the Cryogenic Optical Bench (COB) at the KPNO 4 m telescope were obtained UT 1995 September 5 at a plate scale of 0.″1 pixel^{-1}. Newly deployed real-time shift-and-add capability provided postdetection tip/tilt correction to the output frames which consisted of 256 individual 100 ms images. The combination of fast read time and small pixel scale allowed nonsaturated images to be obtained despite the use of a 4 m telescope. The resultant COB images (an example of which is shown in the insert to Fig. 1) show that objects A, B, and C are unresolved and stellar at the 0.″2 level. Photometry of the COB *K*-band images is consistent with the IRCAM results (Table 3).

TABLE 1

COORDINATES

Source	R.A. (2000)	Decl. (2000)
Object A	19 07 15.34 ± 0.04	+09 19 21.7 ± 0.2
Object B	19 07 15.12 ± 0.04	+09 19 21.0 ± 0.2
Center AB	19 07 15.23 ± 0.04	+09 19 21.4 ± 0.2
IRAS PSC/HIRAS.....	19 07 15.2 ± 0.4	+09 19 20 ± 5
ROSAT HRI	19 07 14.2 ± 0.7	+09 19 19 ± 10

NOTE.—Units of right ascension are hours, minutes, and seconds, and units of declination are degrees, arcminutes, and arcseconds.

In the main panel of Figure 3 we show the spectra of objects A, B, and C, along with the A/B spectral ratio, between 6600 and 8800 Å taken on UT 1995 April 3 with the CTIO 4 m RC spectrograph using a Loral 3k CCD and 1.″5 slit. These data show that the A and B spectra are

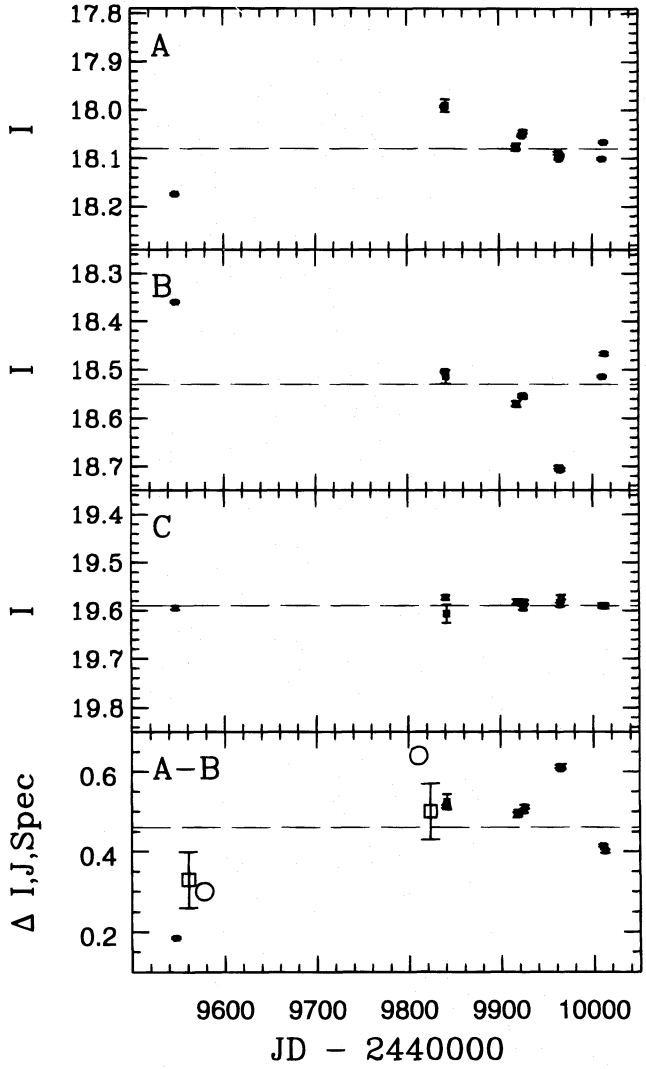

FIG. 2.—The *I*-band CCD photometry obtained at the USNO 1.55 m telescope are plotted as solid squares for objects A, B, and C in the top three panels. The error bars show the standard deviations of multiple frames taken during each night of observing. The dashed lines are the mean values of the photometry for reference. The bottom panel displays the A and B magnitude differences with the same symbols. Overlain on this panel are the A and B magnitude differences for the *J*-band IRCAM photometry of Table 3 (*open squares*) and the *I*-band portions of the spectra (*open circles*) described in § 2.

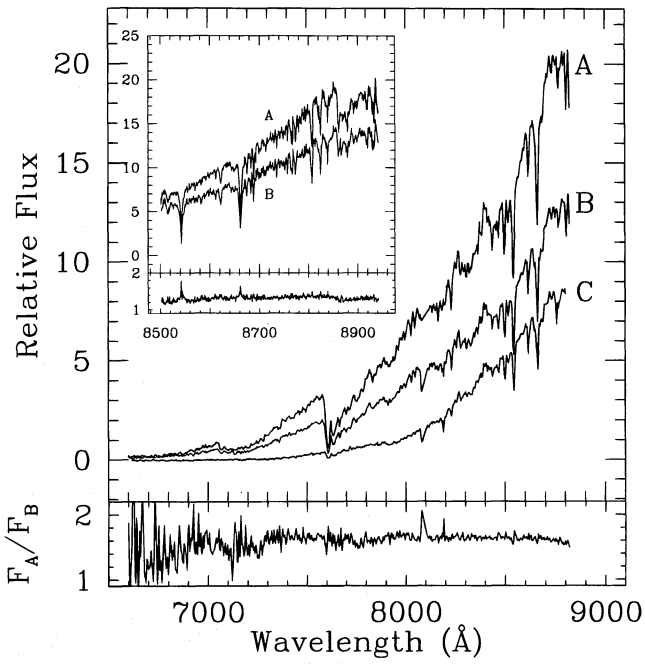

FIG. 3.—The spectra of objects A, B, and C along with the A/B spectral ratio taken with the CTIO 4 m telescope RC spectrograph using a Loral 3k CCD and 1".5 slit are shown in the main panel. The apparent feature in the A/B ratio at 8090 Å is due to a bad column in the B spectrum. In the insert are shown higher resolution spectra of objects A and B taken with the Hale 5 m double spectrograph along with the A/B spectral ratio. The spectra are remarkably similar, except that object A has slightly weaker Ca II absorption at 8542 and 8662 Å and a slightly stronger TiO 8860 Å band head compared to object B, indicating a slightly later spectral type for A.

identical to within the spectral noise, while C is clearly different. The apparent feature in the A/B ratio at 8090 Å is due to a bad column in the B spectrum. Spectra with comparable resolution obtained UT 1994 August 11 with the Hale 5 m telescope and double spectrograph are very similar. Higher resolution double-spectrograph spectra, obtained on UT 1994 August 13, between 8500 and 8920 Å of A and B are shown in the inset to Figure 3 along with the A/B ratio. While objects A and B have remarkably similar spectra, object A has slightly weaker Ca II absorption at 8542 and 8662 Å and a slightly stronger TiO 8860 Å band head than B, indicating a slightly later spectral type for A.

TABLE 2

SUMMARY OF I_C-BAND OBSERVATIONS

JD−2440000	Object A	Object B	Object C	*A*−*B*
9548.....	18.17 ± 0.01	18.36 ± 0.01	19.59 ± 0.01	0.19 ± 0.01
9841.....	17.99 ± 0.01	18.51 ± 0.01	19.57 ± 0.01	0.51 ± 0.01
9842.....	17.99 ± 0.01	18.52 ± 0.01	19.61 ± 0.02	0.52 ± 0.02
9918.....	18.08 ± 0.01	18.57 ± 0.01	19.58 ± 0.01	0.49 ± 0.01
9919.....	18.08 ± 0.01	18.57 ± 0.01	19.58 ± 0.01	0.50 ± 0.01
9925.....	18.05 ± 0.01	18.55 ± 0.01	19.60 ± 0.01	0.50 ± 0.01
9926.....	18.05 ± 0.01	18.56 ± 0.01	19.58 ± 0.01	0.51 ± 0.01
9964.....	18.09 ± 0.01	18.70 ± 0.01	19.60 ± 0.01	0.61 ± 0.01
9965.....	18.10 ± 0.01	18.71 ± 0.01	19.59 ± 0.01	0.61 ± 0.01
9966.....	18.09 ± 0.01	18.71 ± 0.01	19.57 ± 0.01	0.61 ± 0.01
10011	18.10 ± 0.01	18.52 ± 0.01	19.59 ± 0.01	0.41 ± 0.01
10013	18.07 ± 0.01	18.47 ± 0.01	19.59 ± 0.01	0.40 ± 0.01

TABLE 3

SUMMARY OF *J*-, *H*-, AND *K*-BAND OBSERVATIONS

JD−2440000	Camera	Object A	Object B	Object C	*A*−*B*
			J (1.22 μm)		
9561.....	IRCAM	9.34 ± 0.06	9.68 ± 0.04	12.55 ± 0.09	0.33 ± 0.07
9824.....	IRCAM	9.29 ± 0.06	9.78 ± 0.04	12.38 ± 0.09	0.50 ± 0.07
			H (1.66 μm)		
9561.....	IRCAM	7.29 ± 0.05	7.66 ± 0.03	11.29 ± 0.09	0.37 ± 0.06
9824.....	IRCAM	7.27 ± 0.05	7.71 ± 0.03	11.30 ± 0.09	0.44 ± 0.06
			K (2.20 μm)		
9561.....	IRCAM	6.32 ± 0.04	6.71 ± 0.06	10.45 ± 0.09	0.39 ± 0.07
9824.....	IRCAM	6.19 ± 0.04	6.66 ± 0.06	10.44 ± 0.09	0.47 ± 0.07
9966.....	COB				0.50 ± 0.01

The *I*-band magnitude differences inferred from the A and B spectra in Figure 3 are plotted in the A-B panel of Figure 2. They are consistent with the values derived from photometry, indicating that the spectra are cleanly separated.

Figure 4 shows the near-IR spectra of objects A, B, and C, along with the A/B spectral ratio, obtained UT 1995 October 6 with the Cryogenic Spectrometer at the KPNO 4 m telescope. With a pixel scale of 0.″36 pixel^{-1} and 0.″8 seeing the components were completely separated within the 2.″5 extraction region used. Although A and B have a remarkably constant brightness difference over the entire wavelength range, B has slightly stronger CO absorption at 2.3 μm. Object C is confirmed to be clearly different from and bluer than either A or B.

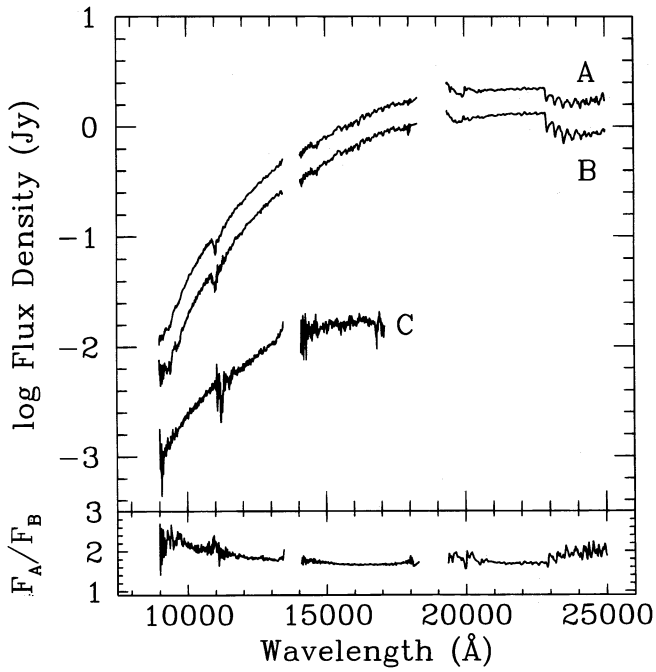

FIG. 4.—The near-infrared spectra of objects A, B, and C, along with the A/B spectral ratio, obtained UT 1995 October 6 with the Cryogenic Spectrometer on the KPNO 4 m telescope are displayed. These spectra show an almost constant brightness difference in the A and B fluxes over the entire wavelength range, except that star B has a slightly stronger 2.3 μm CO absorption. Star C has a clearly different energy distribution.

3. ANALYSIS

Accurate classification of these spectra is difficult due to the extreme steepness of the continua at optical wavelengths and the lack of a grid of spectral standards obtained with the same instrumentation. Nonetheless, comparison with the spectral catalogs of Allen & Strom (1995) and Henry, Kirkpatrick, & Simons (1994) can give temperature classifications to about one spectral subclass using the TiO band head strengths at 7200 Å and 8860 Å, while luminosity information is derived by comparison of the 8807 Å Mg I line with that of Ca II at 8542 and 8662 Å. For this purpose the spectra of objects A and B are indistinguishable and we obtain an M5 I–III classification. The strong CO bands at 2.3 and 1.6 μm are consistent with this classification (Kleinmann & Hall 1986). For object C we obtain M2, but could not obtain a reliable luminosity class as the higher resolution 8500–8940 Å spectrum is rather noisy.

We estimate the interstellar extinction, A_V, to the objects using the $I-J$, $I-H$, and $I-K$ color indices, the range of spectral types determined above, optical and IR intrinsic colors from Johnson (1966) and Koornneef (1983), respectively, and assuming normal interstellar reddening (Johnson 1968). From this we estimate the apparent V magnitudes and, from A_V and M_V (Schmidt-Kaler 1982), the distances to the objects. The results of these calculations are presented in Table 4. We note that the results derived from the different color indices are all consistent within the uncertainties. This result also implies that between 0.80 and 2.2 μm the stars' light is not significantly contaminated by excess emission such as that from hot, dense circumstellar dust.

TABLE 4

PROPERTIES OF OBJECTS A, B, AND C

Object	Spectral Type	A_V (mag)	V_{pred} (mag)	d_{min} (kpc)	d_{mean} (kpc)	d_{max} (kpc)
A.....	M5 I	19.1 ± 1.2	29.0 ± 0.5	7.2	12.6	21.9
	M5 III	19.5 ± 1.0	29.2 ± 0.4	0.6	1.0	1.6
B.....	M5 I	19.2 ± 1.0	29.5 ± 0.4	9.5	15.1	24.0
	M5 III	19.3 ± 1.0	29.5 ± 0.4	0.8	1.3	2.0
C.....	M2 I	15.0 ± 1.2	27.5 ± 0.5	24.0	41.7	72.4
	M2 III	15.4 ± 1.2	27.7 ± 0.4	2.2	3.8	6.6
	M2 V	16.7 ± 1.3	28.4 ± 0.5	0.01	0.02	0.04

We note that, for all spectral cases, stars A and B have similar extinctions exceeding 19 mag, while star C has an extinction of several magnitudes less. The estimated V magnitudes for all cases are consistent with our failure to detect A, B, or C at the $V = 24.5$ detection limit. The mean, minimum, and maximum distances are based on the values of A_V and its 1 σ error bars. The large spread of possible distances at a given spectral type demonstrates the difficulty of distance determination for heavily extinguished objects. Nonetheless, we can greatly restrict the possible distances to all of these stars.

The distances to both A and B are estimated to be 13–15 kpc if they are supergiants, and 1.0–1.3 kpc if they are giants. The associated A_V's are consistent with normal interstellar reddening in the former case but would require a significant component of circumstellar dust obscuration in the latter, which we have argued above is unlikely. A mean absorption of 1.6 mag kpc^{-1} (Allen 1973) in the Galactic plane predicts a distance of $\approx$12 kpc. At Galactic coordinates $l^{II} = 43\overset{\circ}{.}0$, $b^{II} = 0\overset{\circ}{.}76$, the line-of-sight vector extends for about 7 kpc along the Sagittarius spiral arm, crosses an interarm region between 7–13 kpc, and crosses an outer arm defining the gaseous edge of the Galaxy at $\approx$13–15 kpc (e.g., Liszt 1985; Weaver 1974). These considerations place stars A and B at a distance between 12 and 15 kpc.

As a way to verify this, we have carried out astrometric solutions (based on the 30 I-band photometric CCD frames taken over a 1.3 yr time baseline) to find proper motion between stars A and B and the stars marked "J," "M," and "R" in Figure 1. We find a proper motion of 75 $\pm$ 23 mas yr^{-1} between A and B and stars J and R. The vector of this proper motion is along the Galactic plane such that J and R are moving toward smaller Galactic l^{II} with respect to much more distant objects as predicted by the Oort approximation to local Galactic rotation at this l^{II}. This implies $d \gg 1$ kpc for stars A and B and helps to rule out the luminosity class III possibility. We conclude that stars A and B are M5 I stars at a distance of $\approx$12–15 kpc. Star M does not have proper motion with respect to A and B and thus is also $\gg$1 kpc.

Star C has no relative proper motion with respect to stars A and B, thus also likely placing it at $d \gg 1$ kpc and ruling out the distance of 0.01–0.04 kpc implied by a dwarf luminosity class. Also, the extinction value of $A_V \approx 16.7$ mag is untenable at this distance. The distances implied by a class I luminosity would place star C well outside the Galaxy. In addition, it is difficult to reconcile a larger distance, but smaller extinction, for C with respect to A and B. Thus, star C is most likely M2 III, placing it within the Sagittarius spiral arm. The maximum extinction rate of $A_V = 1.9$ mag kpc^{-1} (Allen 1973) would imply $d \approx 8$ kpc; a distance where the line of sight diverges from the Sagittarius arm. This is consistent with the picture that much of the extinction to stars A and B occurs within the nearest 8 kpc. Clearly, star C cannot be much closer than 8 kpc or else it would be difficult to explain the only 4 mag A_V difference between stars A and B, and C. We conclude that C is a foreground star at a distance of $\approx$6–8 kpc, and unrelated to stars A and B.

4. DISCUSSION

The distance of 12–15 kpc and $l^{II} = 43\overset{\circ}{.}0$, $b^{II} = 0\overset{\circ}{.}76$, places stars A and B at the edge of the Galaxy with distance above the Galactic plane of $z = 160$–200 pc. Even at the minimum distance of 7–10 kpc (Table 4), the resultant $z = 90$–130 pc is somewhat large for supergiants, for which the scale height $\approx$50 pc. While one such star at this z would be fairly rare, the fact that we find two such stars in close angular proximity argues strongly that they are gravitationally bound. We have used the Galactic structure models of Mendez (1995) to calculate the probability of a random M5 I star to be located with 3$\overset{''}{.}$4 of another. At their Galactic coordinates and observed apparent magnitudes the probability is less than 6×10^{-8}. We thus conclude that stars A and B are gravitationally bound. At a distance of 12–15 kpc, the angular separation implies a minimum separation $r \geq 0.20$–0.25 pc. For a circular orbit in the plane of the sky, the orbital period would be greater than 2×10^6 yr. The relative motion would be less than 13 μas yr^{-1}, far less than our detection limit of $\approx$10 mas yr^{-1}.

Figure 5 displays the $IJHK$ flux densities of stars A and B (and C for comparison) as well as blackbody curves for the appropriate stellar temperatures and reddened by the observed A_V's. In addition, it shows the flux densities obtained with TIMMI at 10 μm and with HIRAS at 12.5, 25, and 60 μm from van Paradijs et al. (1996). We also plot

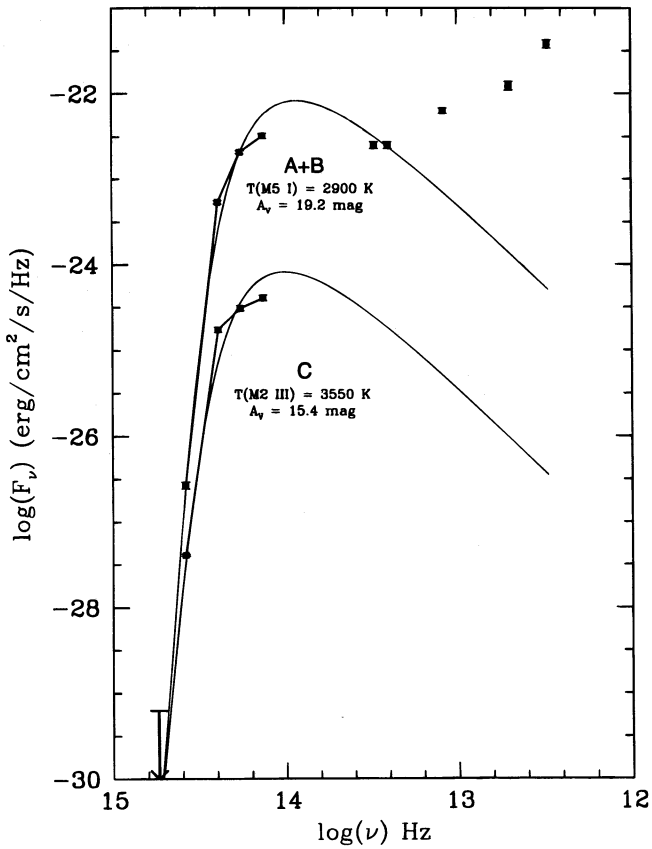

FIG. 5.—The combined $IJHK$ flux densities of stars A and B (and C for comparison) are plotted as a function of log ν. The solid curves are blackbody functions for the appropriate stellar temperatures, reddened by the observed A_V's (not including the interstellar absorption feature near 10 μm), and fitted to the mean J, H, K fluxes. In addition, we have plotted the flux densities at 10 μm obtained with TIMMI and at 12.5, 25, and 60 μm from HIRAS (van Paradijs et al. 1996). We also plot the less-reliable 100 μm flux density from the *IRAS* PSC. The figure demonstrates that the energy distribution of stars A and B is consistent with reddened photospheric emission between 0.55 and 12.5 μm, but not at longer λ.

the less-reliable flux density at 100 μm from the *IRAS* PSC. The figure demonstrates that the energy distribution of stars A and B is consistent with reddened photospheric emission only between 0.55 and 12.5 μm. If we assume that A_V is exactly the same for each star, then their *IJHK* color differences imply that star B is about one-tenth of a spectral subtype earlier then A; consistent with the spectral differences. The lack of IR excess out to 12.5 μm shows the absence of significant hot dust in close proximity to the stars, consistent with our COB observations showing A and B unresolved to $\approx 0\farcs2$. van Paradijs et al. (1996) show that the *IRAS* source is pointlike at 12.5 and 25 μm, but clearly extended at 60 μm. The source apparently peaks in the far-IR as it is not detected at submillimeter wavelengths or beyond (Smith, Chernin, & Hurley 1996). If the far-IR emission is due to dust, one envisions a compact (unresolved) region of warm dust embedded in an extended region of cool dust detected at longer wavelengths. This scenario might be consistent with a history of long-term mass loss from stars A and B, as is often seen from supergiants. However, it cannot explain the strong X-ray source (Vasisht et al. 1994; Hurley et al. 1995, 1996) in this direction.

While there is no known counterpart to SGR 0525−66, originating in the LMC, it is of use to compare and contrast details of the A-B region to those found for the putative counterpart to the other known Galactic SGR: 1806−20. In that case, a heavily extinguished ($A_V \approx 28$ mag) massive O9–B2 supergiant star at a distance of ≥ 6 kpc is associated with the SGR (van Kerkwijk et al. 1995). This star is also at the position of a strong quiescent X-ray source (Murkami et al. 1994) and an *IRAS* source (van Paradijs et al. 1996) where the infrared emission is also unresolved at 25 μm and shorter wavelengths, but extended at 60 μm. Near-IR observations of the O9–B2 star (van Kerkwijk et al. 1995) also show no evidence for hot circumstellar dust. A significant difference is that while SGR 1900+14 has no associated radio emission, SGR 1806−20 is associated with the nonthermal radio nebula G10.0−0.3 (Kulkarni et al. 1995), the high-resolution VLA mapping of which shows a unipolar emission source at the SGR position (Vasisht, Frail, & Kulkarni 1995).

For SGR 1900+14 it seems likely that stars A and B are not directly involved as the source of the SGR. However, the unlikely association of two massive orbiting stars with a strong X-ray source, an *IRAS* source, and (putatively) an SGR invokes speculation about an unseen third component of the system, such as a neutron star, as the source of the SGR. We suggest optical or near-IR radial velocity-sensitive spectroscopy of the visible components of both SGR 1900+14 and SGR 1806−20 to detect the presence of unseen objects.

K. C. H. and P. L. are supported by NASA program NAG 5-1560. D. H. H. is supported by NASA grant NAG 5-1578. I. S. is supported by NASA grants NAG 5-1547 and NAG 5-2772. M. H. v. K. is supported by a NASA Hubble Fellowship. We are grateful to B. Paczyński and R. Blandford for useful discussions. We thank N. Buchholz and J. Heim who are responsible for the KPNO COB real-time shift-and-add system.

REFERENCES

Allen, C. 1973, Astrophysical Quantities (London: Athlone)
Allen, L. E., & Strom, K. M. 1995, AJ, 109, 1379
Cline, T., et al. 1982, ApJ, 255, L45
Dickel, J., et al. 1995, ApJ, 448, 623
Hartmann, D. H., et al. 1995, in AIP Conf. Proc. 366, Workshop on High Velocity Neutron Stars, ed. R. E. Rothschild & R. E. Lingenfelter (New York: AIP), in press
Henry, T. J., Kirkpatrick, J. D., & Simons, D. A. 1994, AJ, 108, 1437
Hurley, K., Sommer, M., Kouveliotou, C., Fishman, G., Meegan, C., Cline, T., Boer, M., & Niel, M. 1994, ApJ, 431, L31
Hurley, K., et al. 1995, AIP Conf. Proc. 366, Workshop on High Velocity Neutron Stars, ed. R. E. Rothschild & R. E. Lingenfelter (New York: AIP), in press
———. 1996, ApJ, 464, 342
Johnson, H. L. 1966, ARA&A, 4, 193
———. 1968, in Nebulae and Interstellar Matter, ed. B. M. Middlehurst & L. H. Aller (Chicago: Univ. Chicago Press), 167
Kleinmann, S. G., & Hall, D. N. B. 1986, ApJS, 62, 501
Koornneef, J. 1983, A&A, 128, 84
Kouvelioutou, C., et al. 1993, Nature, 362, 728
———. 1994, Nature, 368, 125
Kulkarni, S. R., Frail, D. A., Kassim, N. E., Murakami, T., & Vasisht, G. 1994, Nature, 368, 129
Kulkarni, S. R., Matthews, K., Neugebauer, G., Reid, I. N., Van Kerkwijk, M. H., & Vasisht, G. 1995, ApJ, 440, L61
Liszt, H. S. 1985, in The Milky Way Galaxy, ed. H. van Woerden, R. J. Allen, & W. B. Burton (Dordrecht: Reidel), 283
Mendez, R. 1995, Ph.D. thesis, Yale Univ.
Murakami, T., Tanaka, Y., Kulkarni, S. R., Ogasaka, Y., Sonobe, T., Ogawara, Y., Aoki, T., & Yoshida, A. 1994, Nature, 368, 127
Norris, J. P., Hertz, P., Wood, K. S., & Kouveliotou, C. 1991, ApJ, 366, 240
Rothschild, R., Kulkarni, S., & Lingenfelter, R. 1994, Nature, 368, 432
Schmidt-Kaler, Th. 1982, in Landolt-Bornstein, New Series, Group VI (New York: Springer), 2b, 449
Smith, I. A., Chernin, L. M., & Hurley, K. H. 1996, A&A, 307, L1
van Kerkwijk, M. H., Kulkarni, S. R., Matthews, K., & Neugebauer, G. 1995, ApJ, 444, L33
van Paradijs, J., et al. 1996, A&A, in press
Vasisht, G., Kulkarni, S. R., Frail, D. A., & Greiner, J. 1994, ApJ, 431, L35
Vasisht, G., Frail, D. A., & Kulkarni, S. R. 1995, ApJ, 440, L65
Weaver, H. 1974, in Galactic Radio Astronomy, ed. F. J. Kerr & S. C. Simonson III (Dordrecht: Reidel), 573